EAM

Institute for Advanced Science,
Social and Sustainable Future
MORALITY BEFORE KNOWLEDGE

Synthesis of gold nanoparticles with allicin to modify boron-doped diamond surface for oxygen sensor applications

Toto Raharto[1,4], Cahya M. Setiyanto[1], Harits A. Ariyanta[2,3], Dinda P. N. Nahda[1], Adinda M. Hani[1], Yoki Yulizar[1], Tribidasari A. Ivandini[1*], and Yasuaki Einaga[5]

[1] Department of Chemistry, Faculty of Mathematics and Natural Sciences (FMIPA), Universitas Indonesia; Depok, 16424, Indonesia

[2] Research Center for Biomass and Bioproducts, National Research and Innovation Agency; Cibinong, West Java, 16911, Indonesia

[3] Department of Pharmacy, Universitas Gunadarma; Depok, 16424, Indonesia

[4] Department of Chemistry, Faculty of Science and Technology, Universitas Teknologi Nusantara; Bogor, West Java, 16158, Indonesia

[5] Science and Technology, Keio University Japan

* Correspondence: ivandini.tri@sci.ui.ac.id

Abstract

Modification of surface of boron-doped diamond (BDD) film with gold nanoparticles (AuNPs) was carried out to increase its catalytic activity for an application as an oxygen sensor. Allicin was isolated from garlic by salting out extraction technique, and then used as the capping agent to synthesize AuNPs as it has a double bond structure that could be reacted to attach the BDD surface under UV light radiation. An average size of AuNPs at around $46,00 \pm 9,06$ nm was obtained, while the modification of the BDD surface by the synthesized AuNPs indicated that the surface of BDD could be covered by gold at around 0.6 % (w/w). Investigation of the AuNPs-modified BDD as a working electrode for the oxygen reduction by using cyclic voltammograms in 0.1 M phosphate buffer solution pH 7 observed a current peak at around -0.45 V (vs. Ag/AgCl). The current of this peak linearly increased proportionally to the dissolved oxygen concentrations ($R2=0.9986$). Moreover, a limit of detection of the dissolved oxygen of 0.12 ppm and limit of quantity 0.41 ppm could be achieved with excellent stability at 6.86% RSD with 6 repetitions and sensitivity at 19.086 µA/ppm indicated that the modified BDD is promising for applications as an oxygen sensor.

Keywords: allicin; boron doped diamond; electrosensor; gold nanoparticle; oxygen sensor

1. Introduction

Dissolved oxygen (DO) is one of the parameters of water quality index. The development of DO sensors is feasible by making use of the electrochemical signals of oxygen reduction on gold-based electrodes (Chee, Nomura, & Karube, 1999; Chee, Nomura, Ikebukuro, et al., 1999; Y. Li et al., 2016; Sánchez-Iglesias et al., 2018). Studies have shown that gold electrodes exhibit high background current, which could be a problem for the limits of detection of DO (Chee, Nomura, Ikebukuro, et al., 1999; Ivandini et al., 2012). It is also reported that modification of carbon-based electrode with small dimensions of gold particles can provide electrodes with not only high sensitivity to oxygen reduction reaction, but also have low background currents (Chee, Nomura, & Karube, 1999; Y. Li et al., 2016; Toghill & Compton, 2010).

Meanwhile, boron-doped diamond (BDD) is established as a superior electrode among other solid electrodes due to its advantages, such as its high inertness and

biocompatibility, which is coming from its sp3 hybridization (Fujimori et al., 1986). In addition, BDD provides exceptional wide potential window and remarkably low background current, which is an important factor for sensor development (Okano et al., 1990). However, BDD is not sensitive to the electrochemical reduction of oxygen, therefore, it is necessary to modify the surface of BDD to increase its sensitivity (Hutton et al., 2009). Furthermore, modifications of BDD with gold particles have been reported (Fujimori et al., 1986; Hutton et al., 2009; Tenne et al., 1993), where better stability of the current responses was claimed to be achieved when the chemical bonds are involved in the modification of BDD (Gunlazuardi et al., 2022).

In this research, the nanoparticle materials were synthesized using green chemistry pathway called phytosynthesis. Compared to alternative methods, this one is preferable due to its environmental benefits, widespread availability, and ease of extraction process. Among them, plants are the preferred choice for phytosynthesis which possess a diverse arsenal of molecules that assist in the creation of nanomaterials (Ariyanta et al., 2021a). Gold nanoparticles were used to increase the active site on the BDD surface by employing allicin as the capping agent. Allicin, a naturally occurring compound found in garlic, is formed by crushing a garlic clove. This process triggers the conversion of alliin, a cysteine sulfoxide compound, by the enzyme alliinase (F. Li et al., 2017; Nguyen et al., 2021; Yulizar et al., 2017).

It was reported that allicin could be successfully extracted from garlic using the salting-out extraction method with an efficiency of 94.17% and purity of 68.4%. The presence of sulfur functional groups, which is expected to interact with gold nanoparticles, makes allicin a suitable capping agent (F. Li et al., 2017; Sánchez-Iglesias et al., 2018; Yulizar et al., 2017). In addition to that, allicin has C double bonds to be reacted to attach the BDD surface. The chemical structure of allicin is shown in Fig. 1(a), while the expected interaction between AuNPs, allicin and BDD is shown in Fig. 1(b). The capping agent is required to stabilize the nanoparticle to prevent the formation of aggregation.
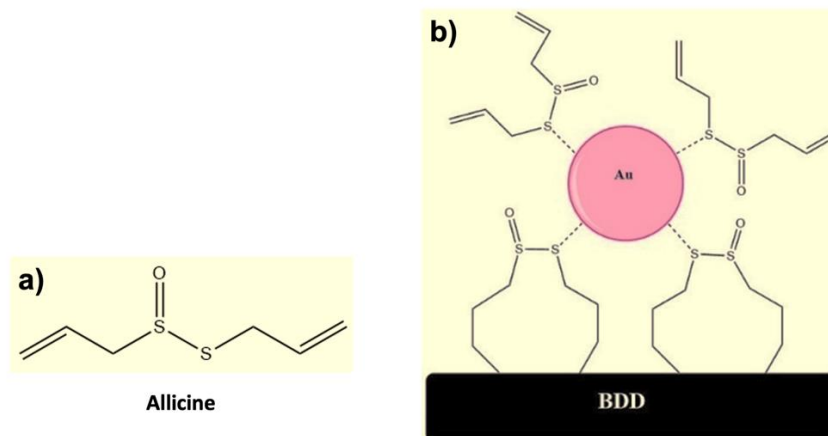
Figure 1. (a) Chemical structure of allicin and
(b) The scheme of the BDD modification using allicin-capped AuNPs

2. Methods

2.1. Materials

The materials used were hydrogen tetrachloroaurate (III) tetrahydrate ($HAuCl_4.4H_2O$) and sodium borohydrate ($NaBH_4$) supplied from Sigma Aldrich, while chloride acid (HCl), K_2HPO_4, KH_2PO_4, 2-propanol and ethanol were obtained from Merck. Garlic (Allium sativum L.) was obtained from the Study Center of Tropical Biopharmaca Bogor Agricultural University, Indonesia. Boron-doped diamond (BDD) films were obtained from Keio University in Japan. The BDD was synthesized in a microwave plasma-assisted chemical vapor deposition system (Cornel Corps.) on Si(100) wafers. As the precursor, methane and B(OCH3)3 were used with a boron-to-carbon ratio of 0.1%. The Raman spectra used to characterize the quality of the BDD showed a peak at 1333 cm−1 attributed to sp3 character

of diamond phase and the absence of peak at around 1500 cm−1 indicated no sp2 impurities in the prepared film (Ivandini & Einaga, 2021; Toghill & Compton, 2010). Prior to modification, the BDD film was cleaned to remove the impurities by subsequently ultrasonication in 2-propanol for 10 min and water.

2.2. Isolation of Allicin with Salting-out Extraction

Isolation of allicin was performed following the previous report (Ariyanta et al., 2021a). About 40 gram of garlic was peeled, smashed into powder, and ground for about 30 min. Then, the garlic powder was treated by ultrasonic-assisted extraction for 20 min using absolute ethanol to obtain the crude extract of allicin. This extract was further treated with salting-out extraction by adding ammonium sulfate concentration of 23% (w/w) and ethanol concentration of 24% (w/w) (Ariyanta et al., 2021b). Allicin was extracted into the top phase (organic solvent-rich phase), while some hydrophilic substances, such as alliin, lysine, and glutamic, tended to precipitate at the bottom phase (salt-rich phase). After filtering, drying, and washing, the obtained allicin was confirmed by using Fourier Transform Infrared (FT-IR) spectroscopy in comparison with the commercial allicin. The similar skeletal spectrum between them was observed indicated the allicin was successfully isolated as shown in Figure 2(d). The peaks at the wavenumber of 2958 cm^{-1}, 2297 cm^{-1}, 1643 cm^{-1}, and 1048 cm^{-1} indicates the presence of Csp^3-H bonds, S-C bonds as well as the stretching vibration of C=C and S=O bond, respectively. In addition, a peak at wavenumber of 3390 cm^{-1} attributed to the asymmetric stretching hydroxyl bond of the solvent was also observed (F. Li et al., 2017).

2.3. Synthesis of Gold Nanoparticles (AuNPs)

The AuNPs were synthesized by mixing 5 mL HAuCl$_4$.4H$_2$O 0.01% (w/v) with various concentrations of allicin from 0.01 – 0.1 % (v/v). Then, the mixture was added by 0.5 mL of 0.1 M NaBH$_4$ and mixed again for 10 min. The characterization was performed by using UV-Vis spectrophotometer BioTek Instrument- Synergy H1MF Microplate Spectrophotometer, transmission electron microscopy (TEM), and particle size analyzer Horiba-SZ 100z Particle Size Analyzer.

2.4. Modification of BDD with AuNPs

The modification of BDD with AuNPs-BDD was performed by immersing the BDD film in the prepared colloidal solution of AuNPs and irradiated under UV light 100 Watt for 6 h. The modified BDD surface was characterized by using Transmission Electron Microscopy (TEM) FEI Tecnai G2 SuperTwin, X-ray photoelectron spectroscopy (XPS) Thermo Fisher Scientific ESCALAB QXi, and cyclic voltammetry using Potentiostat EDAQ-ER466.

2.5. Electrochemical Study of AuNPs-BDD as Oxygen Sensors

The electrochemical study was performed in an electrochemical cell with 3 electrodes system. The prepared AuNPs-BDD was used as the working electrode, while Ag/AgCl as the reference electrode and Pt wire as the counter electrode. The potency of AuNPs-BDD electrode for the oxygen sensors was evaluated by using cyclic voltammetry technique in a potential range from -1.0 V to +1.5 V. A solution of 0.1 M phosphate buffer saline (PBS) pH 7 was used as the electrolyte with various concentrations of the dissolved oxygen, prepared by oxygen bubbling with various times. The concentration of the dissolved oxygen was confirmed by using DO meter (HANA Technology). The comparison was performed between AuNPs-BDD and gold plate electrode as the control.

3. Results and Discussion

3.1. Synthesis of Gold Nanoparticles (AuNPs)

Gold nanoparticles (AuNPs) were synthesized with allicin as a capping agent that characterized with UV-Vis spectrophotometers in the wavelength range of 300-800 nm as shown in Figure 2(a). After adding NaBH$_4$ solution, the solution changed color from yellow to red wine which indicated the gold ion reduced to AuNPs. The peak at wavelength range

510 – 580 nm indicated that the gold nanoparticles have been formed (Gunlazuardi et al., 2022; Ivandini et al., 2012, 2021). The morphology of the prepared AuNPs is spherical gold nanoparticles, as indicated by maximum absorption wavelength of around 540 nm. Similar results have been also reported in previous studies for the synthesis of spherical gold nanoparticles (Meen et al., 2013; Yadav et al., 2023).
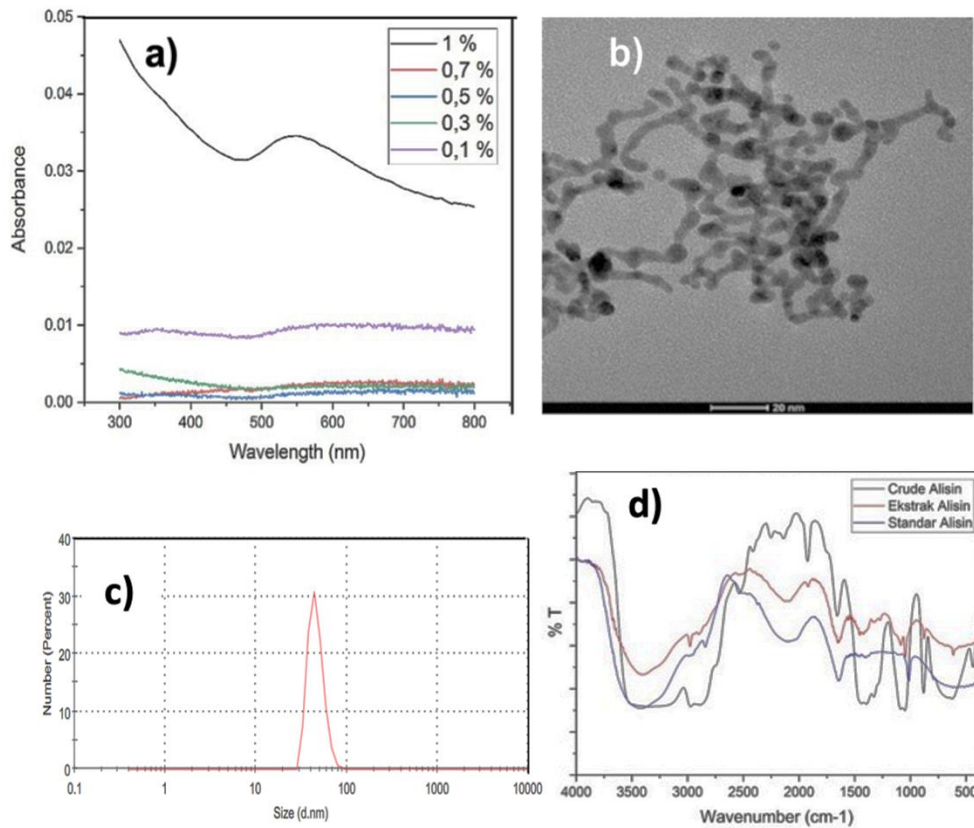
Figure 2 a) UV-Vis Spectrum of AuNPs capping with various concentrations of allicin,
(b) TEM image of AuNPs prepared with 1% allicin,
(c) Percent particle distribution of AuNPs prepared using 1% allicin and
(d) Fourier Transform Infrared (FT-IR) spectra of allicin compared with the commercial allicin

Figure 2(b) shows the results of TEM characterization conducted to determine the morphology and the size of the Au particles that have been successfully formed using the allicin capping agent from garlic extract. The morphology of the spherical gold nanoparticles was also confirmed by TEM results. The formed Au particles have a uniform size surrounded by allicin compounds, as illustrated in accordance with the nanoparticle formation mechanism in Figure 1b. The homogeneity of the Au particles was determined by PSA measurement, where the formation of Au nanoparticles using allicin resulted in a particle size of 46.00 ± 9.064 nm as shown in Figure 2(c).

3.2. *Modification of Boron-doped Diamond Surface with AuNPs*
The surface of BDD was modified with the synthesized AuNPs by immersing the electrode BDD into the colloidal AuNPs under UV irradiation for 6 h. The UV irradiation is necessary to provide energy to destroy the C double bonds to form a chemical bonding with the surface BDD as expected in Fig. 1(b).
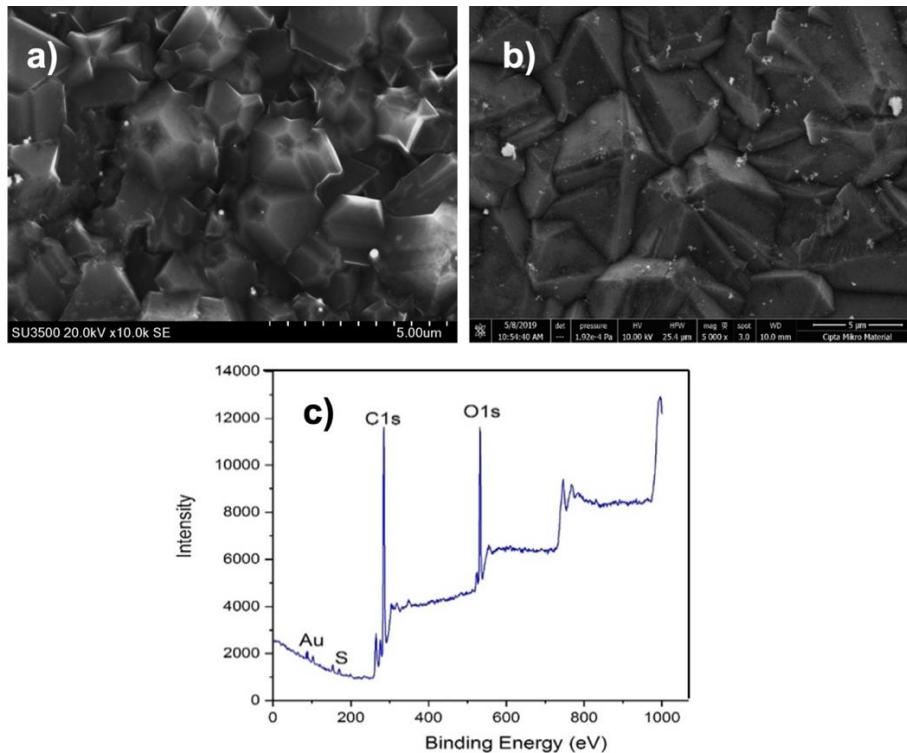
Figure 3 SEM image (a) BDD bare, (b) AuNPs-modified BDD and
(c) XPS spectra of AuNPs-modified BDD

The morphology of the unmodified BDD and AuNPs-modified BDD (AuNPs-BDD) examined with SEM showed the gold as brighter spots on the surface of BDD (Figure 3(b)) compared with the unmodified BDD on Figure 3(a). Meanwhile, the XPS spectra in Figure 3(c) showed typical peaks of BDD for C1s atomic binding energy at 285 eV and atomic O1s at 532 eV. This peak has a very high intensity because the peaks as the surface BDD mainly composed of carbon and oxygen. Beside this peak, gold peaks at binding energy around 89 eV related to Au 4f7/2 and 4f5/2 also observed. In addition, sulfur peak at 153 eV which was associated with S 2p^3/2 was found to indicate the presence of allicin in the AuNPs-BDD electrode prepared(Ariyanta et al., 2021a; Ivandini et al., 2012).
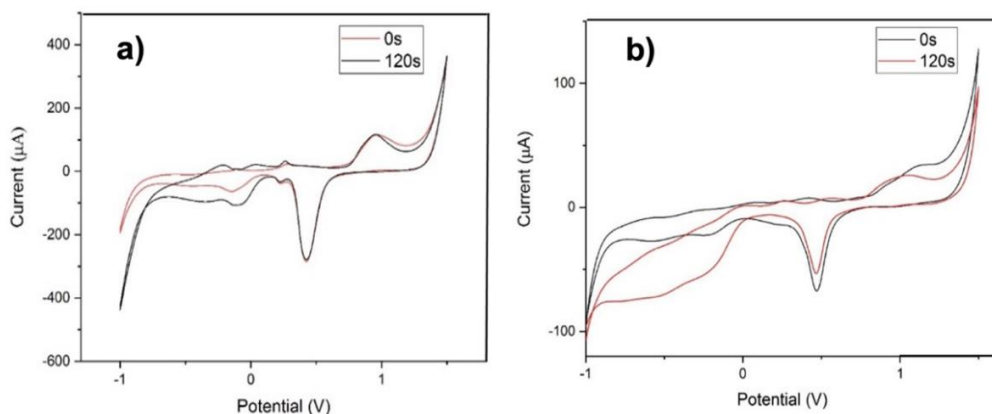
Figure 4. Cyclic voltammogram of 0.1 M phosphate buffer solution pH 7 in the presence of the dissolved oxygen at (a) Gold and (b) AuNPs-BDD electrodes. The scan rate was 100 mV/s.

Cyclic voltammetry was carried out in 0.1 M PBS pH 7 to show the presence of AuNPs on the surface BDD. Voltammogram comparison in the potential range from -1 to +1.5 V (Vs. Ag/AgCl) in gold electrode (Figure 4a) and AuNPs-BDD electrode (Figure 4b). Characteristic peak of gold oxidation at +1.1 V and peak reduction at +0.46 V both appeared on the gold electrode and the AuNPs-BDD electrode which confirmed AuNPs was deposited

on the surface BDD successfully (Chiang et al., 2019). However, the current produced at the AuNPs-BDD electrode is much lower than gold electrode. And it also showed the difference in O2 reduction peak during aeration time which proved that gold electrode and AuNPs-BDD electrode were sensitive to oxygen and can be used as an oxygen sensor.

Table 1. Signal to background ratio of prepared electrodes

Electrode	Background current (μA)	Signal current (μA)	S/B
Au	-11.49	-54.79	4.76
AuNPs-BDD	-8.52	-39.44	4.63

The S/B value is used to determine the ratio of the current signal to the background of an electrode. The higher the S/B value obtained, the better the current separation that can be used to calculate the detection limit. On the Table 1, the prepared electrode of AuNPs-BDD depicted comparable S/B value at 4.63 with the unmodified gold electrode at 4.76. This result imagines that both materials can be used as Oxygen sensors even though the current response from AuNPs-BDD was lower than unmodified gold electrode.

3.3. Electrochemical Study of AuNPs-BDD as Oxygen Sensors

The AuNPs-BDD electrode was measured with the cyclic voltammetry method for oxygen detection. Variations of oxygen aeration time in PBS pH 7 solutions were used as samples for both AuNPs-BDD and gold electrodes. The dissolved oxygen concentration was measured by a dissolved oxygen meter (Hana Technology) as shown in Figures 5(a) and (c). Besides the typical peak of the gold electrode discussed in Figure 4(a) and (b), the voltammogram in Figure 5(a) and (c) showed a peak of oxygen reduction at around −0.1 V and −0.6 V (vs Ag/AgCl). The current generated by this peak increased by the increased oxygen aeration time. The longer aeration would raise the DO concentration in the system. Thus, by plotting the current generated over the increased concentration of DO, the calibration curve of DO can be made as shown in Figure 5(b) and (d).
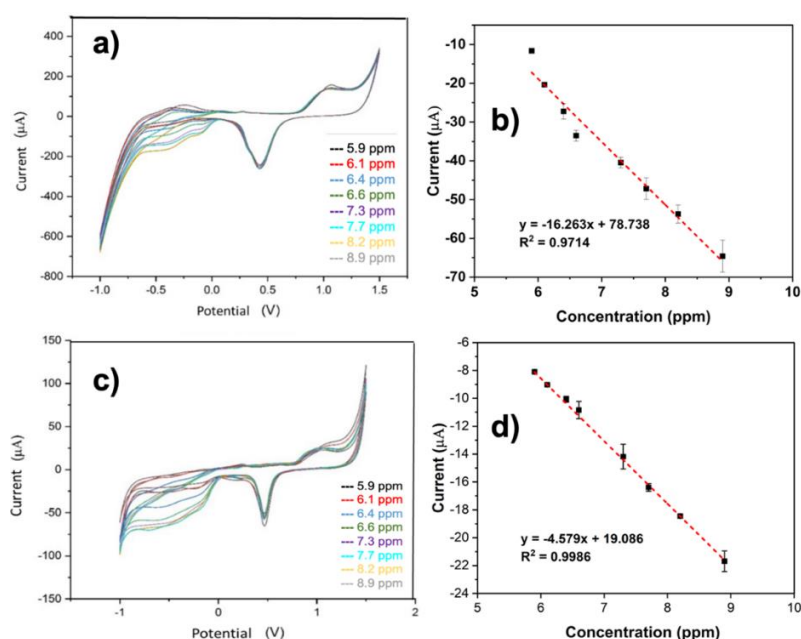
Figure 5. Cyclic voltammogram of various aeration time of dissolved oxygen in PBS 0.1 M pH 7 and linear calibration curve of a-b) Gold electrode and c-d) AuNPs-BDD electrode

The linear equation of y= -4.5785x+19.086 (R2= 0.9986) with a signal to background ratio (S/B) of 4.63 and the limit of detection (LOD) of 0.12 ppm and 0.41 ppm was achieved at AuNPs-BDD electrode. The result is comparable to the gold electrode with

a linear equation y=-16.263x+78.738 (R2=0.9714), S/B ratio 4.76 and LOD 0.55 ppm and LOQ 1.83 ppm. The result showed that the synthesized AuNPs-BDD electrode possible to be applied as oxygen sensors.
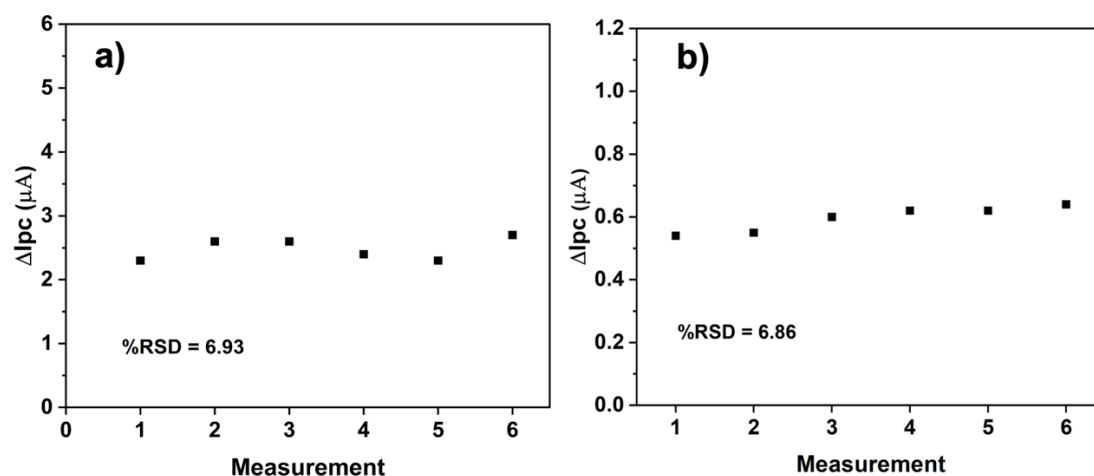
Figure 6. Repeatability test of prepared sensor for oxygen sensor a) gold electrode and b) AuNPs-BDD electrode

Based on the figure, it can be seen that the Au (Figure 6(a)) and AuNPs-BDD (Figure 6(b)) electrodes can work quite well for 6 repetitions with a RSD (Relative Standard Deviation) value of 6.93% on the Au electrode and 6.86% on the AuNPs-BDD electrode. This result indicates that the modification of nanoparticle Au on the surface BDD electrode have slightly better performance in the stability test of DO sensor compared to the monometallic Au electrode. This phenomenon caused by the surface enhancement of the BDD electrode using Au nanoparticle which promote more active surface contact with the oxygen species in the electrochemical sensor measurement which stabilized by allicin as capping agent to maintain the electrode performance in optimum condition. The surface enhancement of BDD electrode resulted good potential performance in the dissolve oxygen detection with favorable limit of detection and highest sensitivity compared to the other noble metal electrode shown on the Table 2. The addition of allicine in the phytosynthesis pathways was successfully inhibit the agglomeration process of gold nanoparticle on the BDD substrate depicted on the higher sensitivity of prepared electrode in the DO measurement.

Table 2. Comparison in developed sensor with other reported oxygen sensors

Electrode	Methods	Linearity range (ppm)	LOD (ppm)	Sensitivity µA/ppm
BDD Patterned sp² (Read et al., 2019)	SWV (-0.55V)	0 – 8.00	-	0.087
LIG/Co-Pt/Nafion/PDMS(Faruk Hossain et al., 2021)	CA (-0.57 V)	0.96 – 12.8	0.077	7.708
GO/Ag (FU et al., 2015)	CA (-0.26 V)	0 – 4.32	0.001	6.406
Ag Wire-type (FU et al., 2015)	CA (-0.55 V)	0 – 55.47	0.950	0.868
PCL/Au (Sanz et al., 2022)	CV (-0.75 V)	2.34 – 9.36	0.450	0.046 x 10⁻³
(Allicine)AuNPs-BDD (This work)	CV (-0.46 V)	5.90 – 8.90	0.120	19.086

SWV = square wave voltammetry, CV = cyclic voltammetry, and CA = chronoamperometry

4. Conclusions

Allicin has been successfully isolated by salting-out extraction technique as indicated by comparing the FTIR characterization with the standard commercial allicin. The use of isolated allicin for the capping agent in the synthesis of gold nanoparticles (AuNPs) produced sphere nanoparticles with the average size of 46.00 ± 9.06 nm. Modification of the

surface with the synthesized AuNPs produced 0.6% (w/w) gold coverage on the BDD surface. Application of the modified BDD electrode for electrochemical study of dissolved oxygen solutions indicated that the modified BDD is not only promising as oxygen sensors with LOD 0.12 ppm and LOQ 0.41 ppm, but also have stable performance with 6.86% RSD value in 6 repetitions and favorable sensitivity at 19.086 µA/ppm.

Acknowledgement

Author Contribution

TR, CMS, YY, and TAI: Conceptualization. data curation, formal analysis, and writing the original draft. TR, HAA, CMS, and YY.: Analysis, validation, writing – review and editing. CMS, HAA, DPNN, and AMH: Data curation and formal analysis. TAI: validation, funding acquisition, and supervisor.

Conflicts of Interest

The authors declare no conflict of interest.

References

Ariyanta, H. A., Ivandini, T. A., & Yulizar, Y. (2021a). Novel NiO nanoparticles via phytosynthesis method: Structural, morphological and optical properties. *Journal of Molecular Structure*, *1227*, 129543. https://doi.org/10.1016/j.molstruc.2020.129543

Ariyanta, H. A., Ivandini, T. A., & Yulizar, Y. (2021b). Poly(methyl orange)-modified NiO/MoS2/SPCE for a non-enzymatic detection of cholesterol. *FlatChem*, *29*, 100285. https://doi.org/10.1016/j.flatc.2021.100285

Chee, G.-J., Nomura, Y., Ikebukuro, K., & Karube, I. (1999). Development of highly sensitive BOD sensor and its evaluation using preozonation. *Analytica Chimica Acta*, *394*(1), 65–71. https://doi.org/10.1016/S0003-2670(99)00289-5

Chee, G.-J., Nomura, Y., & Karube, I. (1999). Biosensor for the estimation of low biochemical oxygen demand. *Analytica Chimica Acta*, *379*(1–2), 185–191. https://doi.org/10.1016/S0003-2670(98)00680-1

Chiang, H.-C., Wang, Y., Zhang, Q., & Levon, K. (2019). Optimization of the Electrodeposition of Gold Nanoparticles for the Application of Highly Sensitive, Label-Free Biosensor. *Biosensors*, *9*(2), 50. https://doi.org/10.3390/bios9020050

Faruk Hossain, M., McCracken, S., & Slaughter, G. (2021). Electrochemical laser induced graphene-based oxygen sensor. *Journal of Electroanalytical Chemistry*, *899*, 115690. https://doi.org/10.1016/j.jelechem.2021.115690

FU, L., ZHENG, Y., FU, Z., WANG, A., & CAI, W. (2015). Dissolved oxygen detection by galvanic displacement-induced graphene/silver nanocomposite. *Bulletin of Materials Science*, *38*(3), 611–616. https://doi.org/10.1007/s12034-015-0900-5

Fujimori, N., Imai, T., & Doi, A. (1986). Characterization of conducting diamond films. *Vacuum*, *36*(1–3), 99–102. https://doi.org/10.1016/0042-207X(86)90279-4

Gunlazuardi, J., Kurniawan, A. D., Jiwanti, P. K., Einaga, Y., & Ivandini, T. A. (2022). Core–shell copper-gold nanoparticles modified at the boron-doped diamond electrode for oxygen sensors. *Analytical Methods*, *14*(7), 726–733. https://doi.org/10.1039/D1AY01942B

Hutton, L., Newton, Mark. E., Unwin, P. R., & Macpherson, J. V. (2009). Amperometric Oxygen Sensor Based on a Platinum Nanoparticle-Modified Polycrystalline Boron Doped Diamond Disk Electrode. *Analytical Chemistry*, *81*(3), 1023–1032. https://doi.org/10.1021/ac8020906

Ivandini, T. A., & Einaga, Y. (2021). Electrochemical Sensing Applications Using Diamond Microelectrodes. *Bulletin of the Chemical Society of Japan*, *94*(12), 2838–2847. https://doi.org/10.1246/bcsj.20210296

Ivandini, T. A., Luhur, M. S. P., Khalil, M., & Einaga, Y. (2021). Modification of boron-doped diamond electrodes with gold–palladium nanoparticles for an oxygen sensor. *The Analyst*, *146*(9), 2842–2850. https://doi.org/10.1039/D0AN02414G

Ivandini, T. A., Saepudin, E., Wardah, H., Harmesa, Dewangga, N., & Einaga, Y. (2012). Development of a Biochemical Oxygen Demand Sensor Using Gold-Modified Boron Doped Diamond Electrodes. *Analytical Chemistry*, *84*(22), 9825–9832. https://doi.org/10.1021/ac302090y

Li, F., Li, Q., Wu, S., & Tan, Z. (2017). Salting-out extraction of allicin from garlic (Allium sativum L.) based on ethanol/ammonium sulfate in laboratory and pilot scale. *Food Chemistry*, *217*, 91–97. https://doi.org/10.1016/j.foodchem.2016.08.092

Li, Y., Sun, J., Wang, J., Bian, C., Tong, J., Li, Y., & Xia, S. (2016). A single-layer structured microbial sensor for fast detection of biochemical oxygen demand. *Biochemical Engineering Journal*, *112*, 219–225. https://doi.org/10.1016/j.bej.2016.04.021

Meen, T.-H., Tsai, J.-K., Chao, S.-M., Lin, Y.-C., Wu, T.-C., Chang, T.-Y., Ji, L.-W., Water, W., Chen, W.-R., Tang, I.-T., & Huang, C.-J. (2013). Surface plasma resonant effect of gold nanoparticles on the photoelectrodes of dye-sensitized solar cells. *Nanoscale Research Letters*, *8*(1), 450. https://doi.org/10.1186/1556-276X-8-450

Nguyen, B. T., Hong, H. T., O'Hare, T. J., Wehr, J. B., Menzies, N. W., & Harper, S. M. (2021). A rapid and simplified methodology for the extraction and quantification of allicin in garlic. *Journal of Food Composition and Analysis*, *104*, 104114. https://doi.org/10.1016/j.jfca.2021.104114

Okano, K., Kurosu, T., Iida, M., Eickhoff, T., Wilhelm, H., & Zahn, D. R. T. (1990). An optical investigation of diamond thin films on silicon. *Vacuum*, *41*(4–6), 1387–1389. https://doi.org/10.1016/0042-207X(90)93965-L

Read, T. L., Cobb, S. J., & Macpherson, J. V. (2019). An sp ^{2} Patterned Boron Doped Diamond Electrode for the Simultaneous Detection of Dissolved Oxygen and pH. *ACS Sensors*, *4*(3), 756–763. https://doi.org/10.1021/acssensors.9b00137

Sánchez-Iglesias, A., Claes, N., Solís, D. M., Taboada, J. M., Bals, S., Liz-Marzán, L. M., & Grzelczak, M. (2018). Reversible Clustering of Gold Nanoparticles under Confinement. *Angewandte Chemie*, *130*(12), 3237–3240. https://doi.org/10.1002/ange.201800736

Sanz, C. G., Mihaila, A. C., Evanghelidis, A., Diculescu, V. C., Butoi, E., & Barsan, M. M. (2022). Quantification of cell oxygenation in 2D constructs of metallized electrospun polycaprolactone fibers encapsulating human valvular interstitial cells. *Journal of Electroanalytical Chemistry*, *905*, 116005. https://doi.org/10.1016/j.jelechem.2021.116005

Tenne, R., Patel, K., Hashimoto, K., & Fujishima, A. (1993). Efficient electrochemical reduction of nitrate to ammonia using conductive diamond film electrodes. *Journal of Electroanalytical Chemistry*, *347*(1–2), 409–415. https://doi.org/10.1016/0022-0728(93)80105-Q

Toghill, K. E., & Compton, R. G. (2010). Metal Nanoparticle Modified Boron Doped Diamond Electrodes for Use in Electroanalysis. *Electroanalysis*, *22*(17–18), 1947–1956. https://doi.org/10.1002/elan.201000072

Yadav, S., Sharma, T., Kaushik, R., & Malhotra, P. (2023). Peroxidase mimicking activity of *Saccharum officinarum* L. capped gold nanoparticles using *o* -dianisidine as a substrate. *New Journal of Chemistry*, *47*(5), 2372–2382. https://doi.org/10.1039/D2NJ05278D

Yulizar, Y., Ariyanta, H. A., & Abduracman, L. (2017). Green Synthesis of Gold Nanoparticles using Aqueous Garlic (Allium sativum L.) Extract, and Its Interaction Study with Melamine. *Bulletin of Chemical Reaction Engineering & Catalysis*, *12*(2), 212–218. https://doi.org/10.9767/bcrec.12.2.770.212-218